Achievable roll stability of heavy road vehicles

D J M Sampson and **D Cebon***
Cambridge University Engineering Department, Cambridge, UK

Abstract: A general purpose numerical model, suitable for simulating the yaw–roll behaviour of torsionally flexible heavy goods vehicles with an arbitrary arrangement of vehicle units, is presented. A controllability analysis is then performed to examine the fundamental limitations in achievable roll stability of heavy vehicles with active roll control systems. It is established that it is not possible to control simultaneously and independently all axle load transfers and body roll angles. The best achievable control objective for maximizing roll stability is shown to be setting the normalized load transfers at all critical axles to be equal, while taking the largest inward suspension roll angle to the maximum allowable angle. The results of a simulation of a tractor–semitrailer vehicle with a full-state feedback active roll control system are presented. It is shown that the roll stability of the vehicle can be increased by 30–40 per cent for steady state and transient manoeuvres and that the handling performance improves significantly.

Keywords: heavy vehicle, rollover, active roll control, active suspension

NOTATION

a	longitudinal distance to the axle, measured forwards from the centre of the sprung mass
a'	longitudinal distance to the axle, measured forwards from the centre of the total mass
a_y	lateral acceleration
A, **B**, **C**, **D**	state space matrices
b	longitudinal distance to the articulation point, measured forwards from the centre of the sprung mass
b'	longitudinal distance to the articulation point, measured forwards from the centre of the total mass
c_1, c_2	tyre cornering stiffness coefficients, in the equation $F_y/\alpha = c_1 F_z + c_2 F_z^2$
c_α	tyre cornering stiffness, measured at the rated vertical tyre load
d	track width
F_y	lateral tyre force
F_z	vertical tyre force
g	acceleration due to gravity
G	plant transfer function
h	height of the centre of the sprung mass, measured upwards from the roll centre
h_a	height of the articulation point, measured upwards from the ground
h_{cm}	height of the total centre of the mass, measured upwards from the ground
h_s	height of the centre of the sprung mass, measured upwards from the ground
h_u	height of the centre of the unsprung mass, measured upwards from the ground
$I_{x'x'}$	roll moment of inertia of the sprung mass, measured about the origin of the (x', y', z') coordinate system
$I_{x'z'}$	yaw–roll product of inertia of the sprung mass, measured about the origin of the (x', y', z') coordinate system
$I_{z'z'}$	yaw moment of inertia of the total mass, measured about the origin of the (x', y', z') coordinate system
k	suspension roll stiffness
k_t	tyre roll stiffness
K	controller transfer function
l	suspension roll damping rate
m	total mass
m_s	sprung mass
m_u	unsprung mass
N_β	partial derivative of the net tyre yaw moment with respect to the side-slip angle $= \partial M_z/\partial\beta = \sum_j a'_j c_{\alpha,j}$
N_δ	partial derivative of the net tyre yaw moment with respect to the steer angle $= \partial M_z/\partial\delta = -a'_1 c_{\alpha,1}$

The MS was received on 9 January 2002 and was accepted after revision for publication on 13 December 2002.
** Corresponding author: Cambridge University Engineering Department, Trumpington Street, Cambridge CB2 1PZ, UK.*

$N_{\dot{\psi}}$	partial derivative of the net tyre yaw moment with respect to the yaw rate $= \partial M_z/\partial\dot{\psi} = \sum_j a_j'^2 c_{\alpha,j}/U$
r	height of the roll axis, measured upwards from the ground
s	Laplace variable
$\boldsymbol{u}$	active roll torque
U	forward speed
$\boldsymbol{x}$	state vector
x'	longitudinal distance, measured forwards from the centre of the total mass
$\boldsymbol{y}$	measurement output
y'	lateral distance, measured to the right from the vehicle unit centre-line
Y_β	partial derivative of the net tyre lateral force with respect to the side-slip angle $= \partial F_y/\partial\beta = \sum_j c_{\alpha,j}$
Y_δ	partial derivative of the net tyre lateral force with respect to the steer angle $= \partial F_y/\partial\delta = -c_{\alpha,1}$
$Y_{\dot{\psi}}$	partial derivative of the net tyre lateral force with respect to the yaw rate $= \partial F_y/\partial\dot{\psi} = \sum_j a_j' c_{\alpha,j}/U$
$\boldsymbol{z}$	performance output
z'	vertical distance, measured downwards from roll axis
α	tyre slip angle
β	side-slip angle
δ	steer angle
ϕ	absolute roll angle of the sprung mass
ϕ_t	absolute roll angle of the unsprung mass
ψ	heading angle
$\dot{\psi}$	yaw rate

Additional subscripts

f	front
i	ith vehicle unit, or ith vehicle coupling, counted from the front
j	jth axle, counted from the front
r	rear

1 INTRODUCTION

1.1 Rollover of heavy vehicles

Several studies have reported that a significant proportion of the serious heavy-vehicle accidents involve rollover. For example, in 1996 and 1997, the US National Highway Traffic Safety Administration documented over 15 000 rollover accidents per year involving commercial heavy vehicles [**1**, **2**].

A review of heavy-vehicle safety by von Glasner considered that, while some rollover accidents involving articulated vehicles were preventable given a sophisticated warning system and a highly skilled driver, the majority could only be avoided by the intervention of advanced active safety systems [**3**]. Winkler *et al.* also noted that it is very difficult for truck drivers to perceive their proximity to rollover while driving [**4**, **5**].

Winkler *et al.* surveyed US accident statistics and reported a strongly negative correlation between steady state roll stability and the average likelihood of rollover accidents [**4**, **6**, **7**]. The study found that an increase in the static rollover threshold of $0.1g$ in the range 0.4–0.7 caused a 50 per cent reduction in the frequency of rollover accidents for tractor–semitrailer combinations. For example, the average frequency of rollover accidents was 0.16 events per million kilometres travelled among vehicles with a static rollover threshold of $0.5g$ but 0.07 events per million kilometres among vehicles with a static rollover threshold of $0.6g$. The study also established a link between steady state roll stability and the probability of rollover in an accident. Rollover accidents accounted for almost 50 per cent of non-jack-knife accidents to tractor semitrailers with a static rollover threshold of $0.4g$ but less than 15 per cent to tractor–semitrailers with a rollover threshold of $0.6g$. These statistics indicate that, while drivers may drive less stable vehicles more cautiously, they do not change their driving behaviour *enough to compensate fully* for changes in vehicle stability. This is believed to be because drivers are unable to assess rollover stability accurately while driving.

It is clear that even a modest increase in roll stability can lead to a significant reduction in the frequency of rollover accidents.

1.2 Review of previous work

Several workers have investigated the use of active roll control to reduce the body roll of heavy vehicles during cornering [**8**, **9**].

Recently the use of active roll control systems to improve vehicle roll stability and to reduce the likelihood of rollover accidents has been proposed by several authors. Vehicles with conventional passive suspensions tilt out of corners under the influence of lateral acceleration. The centre of sprung mass shifts outboard of the vehicle centre-line and this contributes a destabilizing moment that reduces roll stability. The aim of a stabilizing active roll control system is to lean the vehicle *into* corners such that the centre of sprung mass shifts inboard of the vehicle centre-line and contributes a stabilizing roll moment.

Dunwoody and Froese used simulations to investigate the potential benefits of using an active roll control system to increase the steady state roll stability of a tractor–semitrailer [**10**]. The roll control system

hardware was contained entirely within the trailer unit and consisted of a tiltable fifth-wheel coupling and hydraulic actuators at the trailer axles. The input to the roll controller was a lateral acceleration signal from an accelerometer mounted on the trailer. Controller gains were selected using a steady state roll-plane model. These workers concluded that the system could increase the rollover threshold by 20–30 per cent for a wide range of trailer loading conditions.

Lin *et al.* investigated the use of an active roll control system to reduce the total lateral load response of a single-unit truck to steering inputs [**11**, **12**]. A linear model with four degrees of freedom (yaw, side-slip, sprung mass roll angle and unsprung mass roll angle) was used. A steering input spectrum was derived by considering the low-frequency steering inputs required to follow the road (based on road alignment data) as well as the higher-frequency inputs needed to perform frequent lane change manoeuvres. This spectrum was used to design an optimal full-state linear quadratic controller to regulate load transfer. This control scheme caused the vehicle to lean into corners. The lateral acceleration level at which wheel lift-off was first experienced was increased by 66 per cent and the r.m.s. load transfers in response to a random steering input were reduced by 34 per cent. A proportional–derivative lateral acceleration feedback controller was also designed using pole placement. Although the reductions in total load transfer were smaller, the lateral acceleration controller was attractive because of its simpler instrumentation requirements.

Lin *et al.* also investigated the use of active roll control to enhance the roll stability of a tractor–semitrailer [**11**, **13**]. The design of the roll control system was performed using a seven-degree-of-freedom linear model. The controller used lateral acceleration signals from the tractor and trailer to control active antiroll bars fitted to the tractor and trailer axles. The proportional controller gains were selected for good steady state roll stability and the derivative gains were chosen to equate the normalized r.m.s. load transfers of the two units. The system reduced steady state and transient load transfers by up to 30 per cent. Results were confirmed by time domain simulations using a validated non-linear yaw–roll model [**14**]. These workers noted that the transfer of roll moment across the fifth-wheel coupling allowed the roll control system on the tractor to contribute to the roll stability of the trailer.

1.3 Research needs

This study seeks to identify the nature of fundamental limitations in achievable roll stability for vehicles with active roll control systems. An understanding of these limitations is necessary to enable the formulation of achievable control system design objectives that maximize vehicle roll stability.

2 VEHICLE MODELS

2.1 Single-unit vehicle model

The roll and handling response of a single-unit vehicle to steering inputs was investigated using a linear model that built on models formulated by Segel [**15**] and Lin [**11**]. Pitching and bouncing motions have only a small effect on the roll and handling behaviour of the vehicle and so were neglected. The effects of aerodynamic inputs (wind disturbances) and road inputs (cross-gradients, dips and bumps) were also neglected.

The single-unit vehicle was modelled using four rigid bodies (two to represent the sprung mass, and one each for the front and rear axle groups), as shown in Fig. 1. For vehicles with multiple axles at the rear, these axles were combined to form a single rigid body.

Previous investigations into the use of active roll control systems on heavy vehicles have all used the assumption that vehicle frames are rigid bodies. However, torsional compliance of the vehicle frame influences the distribution of roll moments between axle groups, and significant frame compliance affects roll and handling performance noticeably. Winkler *et al.* noted that 'the torsional compliance of the vehicle frame stands out as a uniquely important element in establishing the roll stability of some vehicles, particularly those with flatbed trailers' [**4**]. It is essential to include the torsional flexibility of the frame in the vehicle model to predict the rollover threshold of such vehicles accurately.

Since the motivation for including the frame flexibility was only to capture the influence of compliance on the distribution of roll moments between axles (and not to model torsional vibration), a simple model of the frame using two rigid bodies was used. The sprung mass was split into front and rear sections, each with appropriate inertial properties. These two sections of the sprung mass were connected with a torsional spring whose stiffness matched the torsional stiffness of the vehicle frame. The torsional spring was sited at the centroid height of the frame, so that the line of action of the lateral shear force in the vehicle frame was properly represented. A small amount of torsional damping, representing the energy dissipation inherent in the structure of the vehicle frame, was also included.

The vehicle was allowed to translate longitudinally and laterally and could yaw. The sprung masses rotated about a horizontal roll axis fixed in the unsprung masses, the location of the roll axis being dependent on the kinematic properties of the front and rear suspensions. The unsprung masses also had a roll degree of freedom, enabling the effect of the vertical compliance of the tyres on the roll performance to be included in the model.

The suspension springs, dampers and antiroll bars generated moments between the sprung and unsprung masses in response to roll motions. The roll stiffness and damping of the vehicle suspension systems were assumed

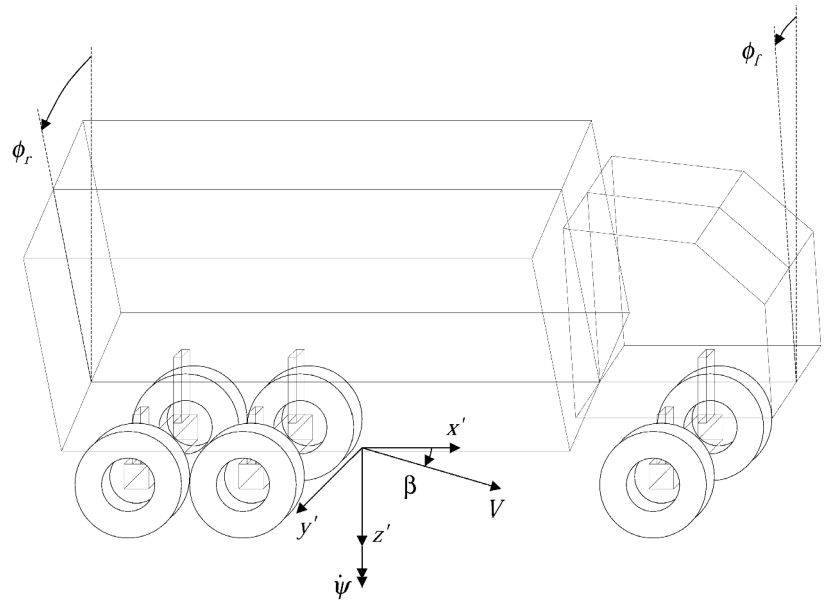

Fig. 1 Single-unit vehicle with flexible frame (ϕ_{f} and ϕ_{r} measured from the vertical). The model has six degrees of freedom: yaw rate $\dot{\psi}$, side-slip angle β, sprung mass roll angles ϕ_{f} and ϕ_{r}, steer axle roll angle $\phi_{\mathrm{t,f}}$ and drive axle roll angle $\phi_{\mathrm{t,r}}$

to be constant for the range of roll motions considered. The active roll control systems at each axle consisted of a pair of actuators and a stiff antiroll bar in parallel with passive springs and dampers. These roll control systems generated additional (controlled) roll moments between the sprung and unsprung masses.

For the purposes of fundamental roll stability analysis (section 3) and control system design (section 4.1), a simplified tyre model with constant cornering stiffness (as a function of both slip angle and vertical load) was used. This assumption of linearity is reasonable for lateral motions of moderate amplitude [**16**]. The effects of aligning moment, camber thrust, roll steer and rolling resistance generated by the tyres are of secondary importance and were neglected.

Further time-domain simulations, including handling analyses (section 4.6), were performed using a non-linear tyre model. The primary source of non-linearity is the variation in tyre cornering stiffness F_y/α with vertical load F_z, and this variation can be described using the quadratic equation

$$\frac{F_y}{\alpha} = c_1 F_z + c_2 F_z^2 \tag{1}$$

This equation is generally suitable for lateral accelerations up to the rollover point and is widely used in heavy-vehicle simulation studies [**17**].

The forward speed of the vehicle was constant during any lateral manoeuvre. (Although forward speed is an important stability parameter, it is not considered to be a variable of motion.)

The equations of motion for the linear single-unit vehicle model are:

$$\begin{aligned} &m_{\mathrm{s,f}} h_{\mathrm{f}} \ddot{\phi}_{\mathrm{f}} + m_{\mathrm{s,r}} h_{\mathrm{r}} \ddot{\phi}_{\mathrm{r}} \\ &\quad = -\, mU(\dot{\beta} + \dot{\psi}) + Y_\beta \beta + Y_{\dot{\psi}} \dot{\psi} + Y_\delta \delta \end{aligned} \tag{2}$$

$$-I_{x'z',\mathrm{f}} \ddot{\phi}_{\mathrm{f}} - I_{x'z',\mathrm{r}} \ddot{\phi}_{\mathrm{r}} + I_{z'z'} \dot{\psi} = N_\beta \beta + N_{\dot{\psi}} \dot{\psi} + N_\delta \delta \tag{3}$$

$$\begin{aligned} I_{x'x',\mathrm{f}} \ddot{\phi}_{\mathrm{f}} - I_{x'z',\mathrm{f}} \dot{\psi} = {} & m_{\mathrm{s,f}} g h_{\mathrm{f}} \phi_{\mathrm{f}} - m_{\mathrm{s,f}} U h_{\mathrm{f}} (\dot{\beta} + \dot{\psi}) \\ & - k_{\mathrm{f}} (\phi_{\mathrm{f}} - \phi_{\mathrm{t,f}}) - l_{\mathrm{f}} (\dot{\phi}_{\mathrm{f}} - \dot{\phi}_{\mathrm{t,f}}) \\ & - k_{\mathrm{b}} (\phi_{\mathrm{f}} - \phi_{\mathrm{r}}) - l_{\mathrm{b}} (\dot{\phi}_{\mathrm{f}} - \dot{\phi}_{\mathrm{r}}) \\ & - F_{\mathrm{b}} h_{\mathrm{b}} + u_{\mathrm{f}} \end{aligned} \tag{4}$$

$$\begin{aligned} I_{x'x',\mathrm{r}} \ddot{\phi}_{\mathrm{r}} - I_{x'z',\mathrm{r}} \dot{\psi} = {} & m_{\mathrm{s,r}} g h_{\mathrm{r}} \phi_{\mathrm{r}} - m_{\mathrm{s,r}} U h_{\mathrm{r}} (\dot{\beta} + \dot{\psi}) \\ & - k_{\mathrm{r}} (\phi_{\mathrm{r}} - \phi_{\mathrm{t,r}}) - l_{\mathrm{r}} (\dot{\phi}_{\mathrm{r}} - \dot{\phi}_{\mathrm{t,r}}) \\ & + k_{\mathrm{b}} (\phi_{\mathrm{f}} - \phi_{\mathrm{r}}) + l_{\mathrm{b}} (\dot{\phi}_{\mathrm{f}} - \dot{\phi}_{\mathrm{r}}) \\ & + F_{\mathrm{b}} h_{\mathrm{b}} + u_{\mathrm{r}} \end{aligned} \tag{5}$$

$$\begin{aligned} &-r(Y_{\beta,\mathrm{f}} \beta + Y_{\dot{\psi}^{\mathrm{f}}} \dot{\psi} + Y_{\delta^{\mathrm{f}}} \delta) \\ &\quad = m_{\mathrm{u,f}} U (h_{\mathrm{u,f}} - r)(\dot{\beta} + \dot{\psi}) + k_{\mathrm{t,f}} \phi_{\mathrm{t,f}} \\ &\quad - m_{\mathrm{u,f}} g h_{\mathrm{u,f}} \phi_{\mathrm{t,f}} - k_{\mathrm{f}} (\phi_{\mathrm{f}} - \phi_{\mathrm{t,f}}) \\ &\quad - l_{\mathrm{f}} (\dot{\phi}_{\mathrm{f}} - \dot{\phi}_{\mathrm{t,f}}) + u_{\mathrm{f}} \end{aligned} \tag{6}$$

$$\begin{aligned} &-r(Y_{\beta,\mathrm{r}} \beta + Y_{\dot{\psi}^{\mathrm{r}}} \dot{\psi}) \\ &\quad = m_{\mathrm{u,r}} U (h_{\mathrm{u,r}} - r)(\dot{\beta} + \dot{\psi}) + k_{\mathrm{t,r}} \phi_{\mathrm{t,r}} \\ &\quad - m_{\mathrm{u,r}} g h_{\mathrm{u,r}} \phi_{\mathrm{t,r}} - k_{\mathrm{r}} (\phi_{\mathrm{r}} - \phi_{\mathrm{t,r}}) \\ &\quad - l_{\mathrm{r}} (\dot{\phi}_{\mathrm{r}} - \dot{\phi}_{\mathrm{t,r}}) + u_{\mathrm{r}} \end{aligned} \tag{7}$$

The notation is detailed at the beginning of the paper.

Equation (2) is a lateral force balance for the entire vehicle. Equation (3) is a yaw moment balance for the entire vehicle. Equations (4) and (5) describe the balance of roll moments on the sprung masses. Equations (6) and (7) describe the roll motions of the front and rear unsprung masses respectively.

The lateral shear force in the vehicle frame, F_b, is given by

$$F_b = (Y_{\beta,f}\beta + Y_{\dot{\psi}^f}\dot{\psi} + Y_{\delta^f}\delta) - m_f U(\dot{\beta} + \dot{\psi}) - m_{s,f}h_f\dot{\phi}'_f \tag{8}$$

These equations can more conveniently be expressed using a state space representation, which is suitable for linear systems analysis and for numerical integration:

$$\dot{\boldsymbol{x}} = \mathbf{A}\boldsymbol{x} + \mathbf{B}_0\boldsymbol{u} + \mathbf{B}_1\delta \tag{9}$$

where $\boldsymbol{x}$ is the state vector given by

$$\boldsymbol{x} = [\beta \quad \psi \quad \phi_f \quad \dot{\phi}_f \quad \phi_r \quad \dot{\phi}_r \quad \dot{\phi}_{t,f} \quad \phi_{t,r}]^T \tag{10}$$

$\boldsymbol{u}$ is the vector of control torques at the active antiroll bars given by

$$\boldsymbol{u} = [u_f \quad u_r]^T \tag{11}$$

and δ is the input steering angle.

2.2 Multiple-unit vehicle model

Models of multiple-unit articulated heavy vehicles can be assembled using modified versions of the single-unit equations of motion presented in Section 2.1 (see reference [**18**] for details). The modifications are necessary to account for the forces and moments applied between adjacent vehicle units through the couplings. An additional equation to describe the kinematic constraint between adjacent vehicle units is required at each coupling:

$$\beta_i - \beta_{i+1} - \frac{r_i - h_{a,r,i}}{U}\dot{\phi}_{f,i} + \frac{r_{i+1} - h_{a,f,i+1}}{U}\dot{\phi}_{r,i+1} + \frac{b'_{r,i}}{U}\psi_i - \frac{b'_{f,i+1}}{U}\psi_{i+1} + \psi_i - \psi_{i+1} = 0 \tag{12}$$

In this way, models of tractor–semitrailers, truck–full-trailers and other long combination vehicles can be derived. Figure 2 shows the model used to investigate the performance of a tractor–semitrailer with a torsionally rigid tractor frame. It had nine degrees of freedom: the five degrees of freedom of the tractor unit (yaw, side-slip, sprung mass roll angle, steer axle roll angle and drive axle roll angle), plus the articulation angle between the tractor and trailer, the roll angle of the sprung section of the trailer, and the roll angle of the trailer axle group.

2.3 Active roll control system model

The active roll control system at an axle group generates a roll moment between the sprung and unsprung masses in response to a demand signal from the controller. Figure 3 shows how the dynamics of the roll control system (as described by the transfer function $\mathbf{G}_{arcs}$ from the moment demanded to the moment generated) affect the closed-loop dynamics of the controlled vehicle.

3 ACHIEVABLE ROLL STABILITY

3.1 The rollover threshold

For a vehicle travelling on a level paved highway, the main inputs that can cause rollover are the lateral forces on the tyres during cornering. The effects of cross winds,

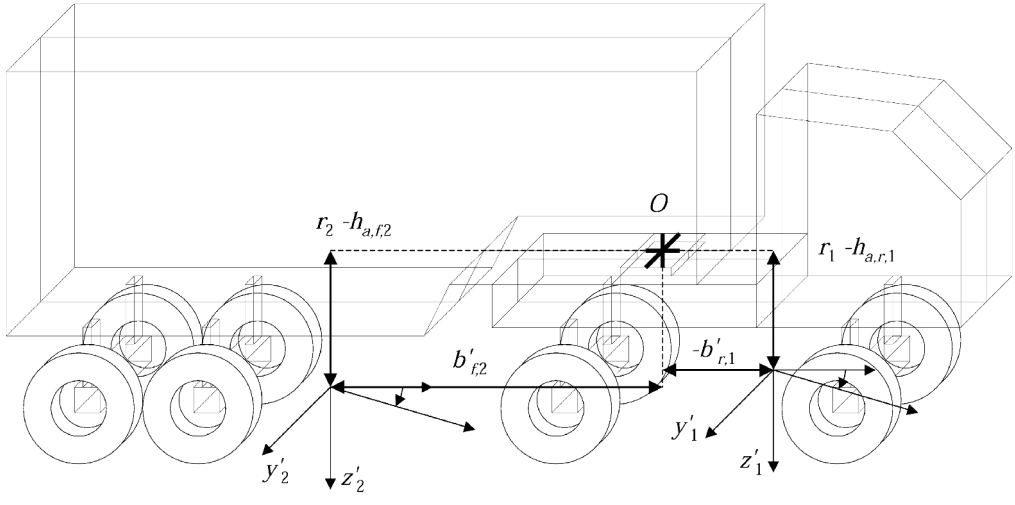

Fig. 2 Coordinate systems used to describe the kinematic constraint at vehicle couplings. The model has three degrees of freedom in addition to those listed in Fig. 1: articulated angle Γ between the tractor and trailer, trailer sprung mass roll angles $\phi_{f,2}$ and $\phi_{r,2}$ and trailer axle roll angle $\phi_{t,r,2}$

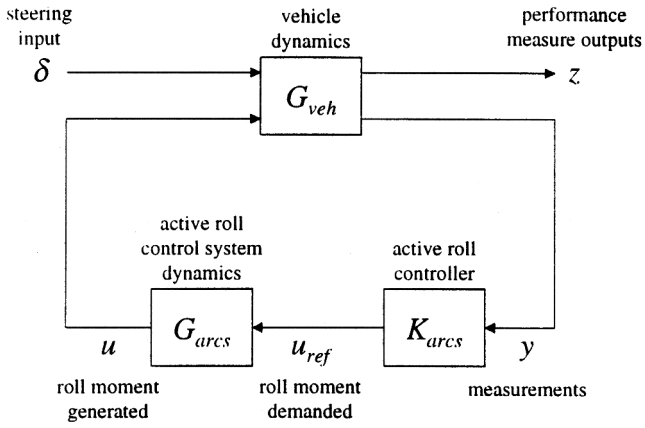

Fig. 3 Active roll control system architecture

excessive road camber and irregularities in the road surface are of secondary importance and are neglected here. The accepted method for static quantifying roll stability is to use the *rollover threshold*, which is the limit of steady state lateral acceleration that a vehicle can sustain without losing roll stability.

Accident statistics for heavy vehicles show a strong correlation between low static roll stability (i.e. low rollover threshold) and the likelihood of being involved in a rollover accident [**16**]. Although it is clear that both static and dynamic effects influence roll stability, a steady state analysis of the roll stability gives useful insight into the major elements governing the roll response of the vehicle.

3.2 Mechanics of rollover

The fundamental mechanics of the rollover process can be investigated using simplified vehicle models.

3.2.1 Simplified suspended vehicle

Firstly, consider a vehicle suspended on compliant passive suspensions and tyres, as shown in Fig. 4. Initially it is convenient to assume that the total mass of the vehicle is in the sprung mass, that the compliance of the suspensions and tyres is lumped into a single equivalent compliance and that the roll of the sprung mass on the tyres and suspension springs takes place about the point on the ground plane at the mid-track position [**16**].

The lateral tyre forces generated at the ground during cornering produce a steady state lateral acceleration of the vehicle. Taking moments about the point on the ground plane at the mid-track position gives

$$ma_y h_{\mathrm{cm}} = \Delta F_z\, d - mgh_{\mathrm{cm}}\phi \tag{13}$$

where

(a) the *primary overturning moment* $ma_y h_{\mathrm{cm}}$ is due to the lateral acceleration,
(b) the *restoring moment* $\Delta F_z\, d$ arises from the lateral load transfer from the inside tyres to the outside tyres and
(c) the *lateral displacement moment* $mgh_{\mathrm{cm}}\phi$ is a consequence of the roll motion which displaces the centre of mass laterally from the nominal centre-line of the vehicle.

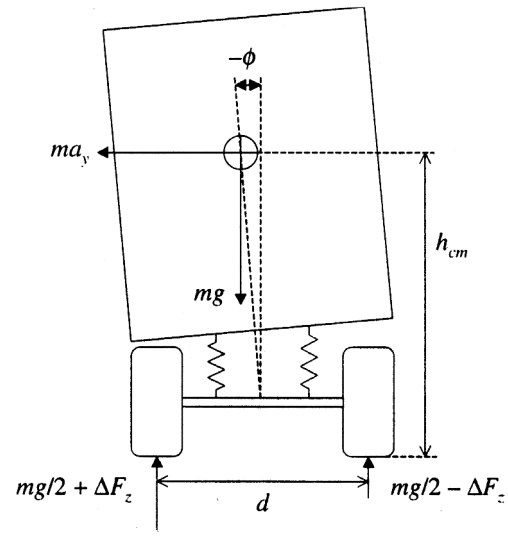

Fig. 4 Simplified suspended vehicle model

The primary overturning moment is a destabilizing moment, and the vehicle will be unstable in roll whenever this moment exceeds the net stabilizing moment that can be provided by the vehicle. For this reason, the analysis of the roll stability of heavy vehicles focuses on the ability of the vehicle to provide a stabilizing moment.

The suspension can only generate a moment by some rolling of the sprung mass. The restoring moment increases linearly with roll angle up to a maximum value of $\frac{1}{2}mgd$. The rollover threshold is then

$$a_y = \frac{dg}{2h_{\mathrm{cm}}} - \phi^* g \tag{14}$$

where ϕ^* is the critical roll angle at wheel lift-off. The rollover threshold is reduced by increasing the roll compliance of the tyres and suspension because stiffer suspensions and tyres cause the lateral displacement moment at wheel lift-off to decrease.

In reality, the sprung mass rolls about a suspension roll centre that is not at ground level, as shown in Fig. 4. The position of the roll centre is determined by the suspension geometry and is generally some distance above the road surface. The unsprung mass rotates about a separate roll centre in the ground place. In general, a higher roll centre will promote less body roll (and correspondingly less lateral displacement of the centre of gravity) and more tyre roll. Since the tyres are significantly less compliant in roll than the suspensions, increasing the suspension roll centre height will typically increase the overall roll stability of the vehicle.

3.2.2 *Suspended vehicle with multiple axles*

To extend the discussion of the mechanics of rollover further, consider a vehicle suspended on multiple compliant suspensions and tyres. The balance between the primary overturning moment and the net restoring moment can be represented on a *roll response graph*, as shown in Fig. 5. This graph is a useful tool for understanding the roll stability of heavy vehicles [**16**]. The primary overturning moment is plotted against lateral acceleration on the left-hand side of the graph. The *net restoring moment*, which is the sum of the restoring moment and the lateral displacement moment, is plotted against roll angle on the right-hand side of the graph.

In this example, the trailer axle has the highest stiffness–load ratio, followed by the tractor drive axle and the tractor steer axle. The trailer axle group is also the most heavily laden, again followed by the tractor drive axle and the tractor steer axle.

For a given track width, the more heavily laden the axle, the greater is the maximum restoring moment that it can provide. Thus the maximum suspension moment that can be supplied is higher for the trailer axle group (point A) than for the tractor drive axle (point B) or the tractor steer axle (point C).

The roll angle at wheel lift-off for a given axle is dictated by the ratio of effective roll stiffness to vertical load, such that axles with a higher stiffness–load ratio lift off at smaller roll angles. Thus the roll angle at which the trailer axle group lifts off (point A) is lower than the corresponding angles for the tractor drive axle (point B) or the tractor steer axle (point C).

The net restoring moment is the sum of the suspension moments and the lateral acceleration moment. Up to point D, all suspensions contribute a moment proportional to the body roll angle and the multiple axle vehicle model behaves identically to the simplified model in section 3.2.1. At point D, the inside tyres of the trailer axle group lift off. The slope of the net restoring moment is reduced beyond D because the trailer axles cannot provide any additional moment. At point E, the inside tyres of the tractor drive axle lift off. The slope of the net restoring moment curve decreases again beyond E. Since the tractor steer axle is not sufficiently stiff to provide a restoring moment to balance the lateral displacement moment, the rollover threshold of the vehicle is defined by the lift off of the inside wheel of the tractor drive axle (point E) rather than of the steer axle (point F).

Figure 5 shows that the non-uniformity of the stiffness–load ratios and the resulting non-simultaneous wheel lift-offs reduce the rollover threshold from the value at point G which would be computed using the lumped suspension model presented in section 3.2.1.

It is clear that the distribution of roll stiffness among the suspensions has an important influence on the rollover threshold. An increase in the roll stiffness of the trailer suspension will shift the trailer lift-off point D to the left on the roll response graph but will not affect the vehicle rollover threshold. A decrease in the roll stiffness of the trailer axle will decrease the rollover threshold only if the stiffness–load ratio of the trailer axle is reduced below that of the tractor drive axle, such that the inside wheel of the tractor drive axle lifts off before the inside wheel of the trailer axle.

A change in the roll stiffness of the tractor drive axle will directly affect the rollover threshold, since the lift-off of the inside wheel of the tractor drive axle defines the rollover condition for this vehicle. Increasing the rollover stiffness of the tractor drive axle will increase the

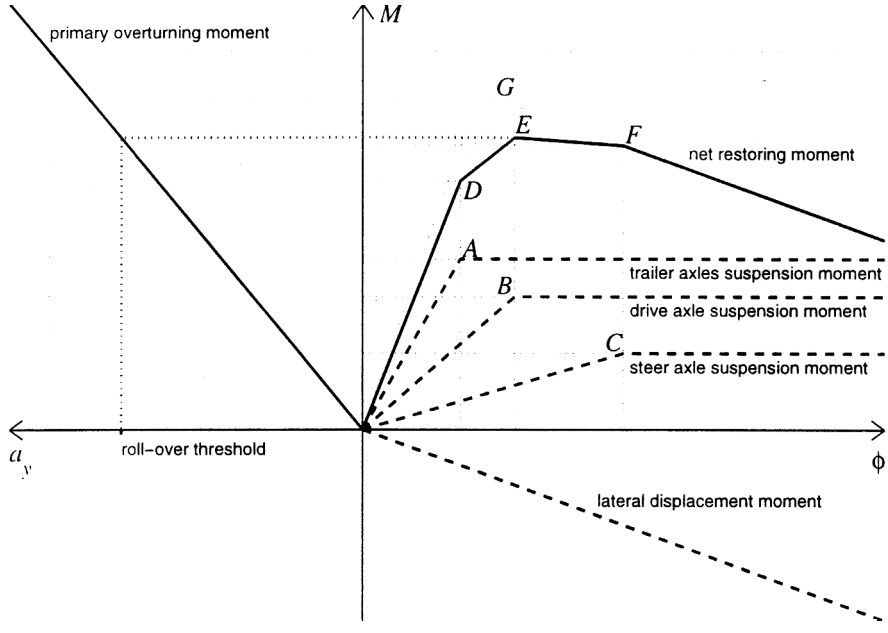

Fig. 5 Generic roll response graph for the suspended vehicle with multiple axles

rollover threshold (moving B to the left and E up and to the left).

The rollover threshold can also be increased by increasing the stiffness of the tractor steer axle. If the steer axle is stiffened to the point where the positive slope of the steer axle roll moment curve is steeper than the negative slope of the lateral displacement moment curve, then the rollover threshold of the vehicle will be determined by the lift-off of the inside wheel of the tractor steer axle (point F) and not the tractor drive axle (point E). This is not normally practical.

3.2.3 *Other factors influencing roll stability*

Torsional compliance of the vehicle frames and couplings also reduces the rollover threshold. For example, a flexible trailer frame rolls to a greater angle under the influence of lateral acceleration, thus increasing the magnitude of the destabilizing lateral displacement moment. Furthermore torsional compliance of the tractor frame reduces the ability of the tractor steer axle to provide a stabilizing moment to resist the roll motion of the payload.

Suspension lash, present in the leaf spring suspension systems commonly used on heavy vehicles, degrades the rollover threshold by reducing the effective roll stiffness of the suspensions.

Winkler *et al.* noted that most real-world rollover accidents feature some dynamic component that raises the vehicle's centre of mass a small distance through its apex height after all axles have left the ground [**4**]. Cooperrider *et al.* investigated the energy required for dynamic rollover and concluded that the lateral acceleration required to achieve rollover in the dynamic case is slightly higher than the static rollover threshold [**19**].

3.3 Controllability analysis

The question of how well it is possible to control the roll motion of a heavy vehicle using active antiroll bars is a question of *input–output controllability analysis*. As applied to the roll control of heavy vehicles, input–output controllability refers to the ability to use torques generated by active antiroll bars to regulate lateral load transfers

$$\Delta F_z = \frac{k_t \phi_t}{d} \tag{15}$$

to below the levels required for wheel lift-off, while also constraining the roll angles between the sprung and unsprung masses ($\phi - \phi_t$) to be within the limits of travel of the suspensions. A maximum suspension roll angle of 6–7° is typical. Roll stability should be maintained despite steering inputs from the driver, deviations from nominal vehicle parameters, and noise in measurements from sensors.

To perform controllability analysis, the vehicle is cast as a multiple-input multiple-output plant of the form

$$\dot{\boldsymbol{x}} = \mathbf{A}\boldsymbol{x} + \mathbf{B}_0\boldsymbol{u} + \mathbf{B}_1\delta, \qquad \boldsymbol{z} = \mathbf{C}_1\boldsymbol{x} \tag{16}$$

The plant inputs are external disturbances (steering δ from the driver) and control inputs (roll moments $\boldsymbol{u}$ generated by active antiroll bars). The internal states $\boldsymbol{x}$ could be, for example, the state variables used in the models in section 2. The performance outputs $\boldsymbol{z}$ are combinations of the vehicle states that are to be controlled in some way.

Controllability is independent of the controller and can only be affected by vehicle design changes. These may include changing the properties of vehicle components, relocating sensors and actuators, adding sensors and actuators or relaxing the control objectives.

Controllability analysis can allow a control system designer to make decisions about actuator placement, sensor placement and the key control objectives to be made *a priori*, without having to perform a detailed controller design. It also allows the limits to achievable roll stability to be quantified.

3.3.1 *Functional controllability analysis*

Functional controllability, which is a necessary condition for input–output controllability [**20**], can be used to determine the maximum number of roll control objectives that may be satisfied using a given arrangement of active antiroll bars.

It is not possible for the number of controlled outputs to exceed the number of control inputs. The roll moment generated by each active antiroll bar (or group of active antiroll bars on a multi-axle suspension group) represents a single control input to the active roll control system. Each axle group also contributes a single output in the form of an unsprung mass roll angle [or equivalently a lateral load transfer, by equation (15)] to the vehicle roll control system. In addition, each vehicle unit contributes either one or two outputs in the form of one or two sprung mass roll angles to the roll control system. Torsionally rigid units contribute one output each, while torsionally flexible units contribute two outputs (one per axle group).

For example, consider the simple case of a single-unit vehicle with a torsionally rigid frame. Such a vehicle has two roll control inputs (one each at the steer and drive axles) and three roll-plane degrees of freedom (the sprung mass roll angle and the lateral load transfers at the steer and drive axles). A tractor–semitrailer combination with a flexible tractor frame will have six roll outputs: the tractor front roll angle, tractor rear roll angle, trailer roll angle, load transfers at the tractor steer axle, tractor drive axle and trailer axle group). This vehicle has three roll control inputs (the active antiroll bar roll moments at the tractor steer axle, tractor drive axle and trailer axle group).

There are not sufficient inputs (active antiroll bar

torques) to control independently all outputs (roll angles and load transfers). Therefore a specification that requires independent controllability of all roll angles and load transfers is not achievable using active antiroll bars alone*. In the case of the torsionally rigid single-unit vehicle, it is possible to control only two of the three roll states:

1. The sprung mass roll angle and the load transfer at the drive axle can be controlled. The load transfer at the steer axle could not then be specified independently.
2. The load transfers at the steer and drive axles can be controlled. The sprung mass roll angle could not then be independently specified.
3. The sprung mass roll angle and the balance of load transfers between the steer and drive axles can be controlled. For example, if the normalized load transfers at the steer and drive axles are set to be the same, so that both axles lift off simultaneously at the rollover threshold, the total load transfer could not then be independently specified.

Functional controllability can be verified numerically as follows. Consider a vehicle in a steady state cornering manoeuvre ($\dot{\boldsymbol{x}} = \mathbf{0}$) under a constant steering input δ. The vehicle is fitted with m active antiroll bars and is required to track m roll control objectives. The equations of motion (9) can be rewritten with the steering input δ and the active antiroll bar torques $\boldsymbol{u}$ stacked to form a single input vector. The state vector $\boldsymbol{x}$ can be partitioned into three parts: the handling states $\mathbf{x}_{\mathrm{h}}$, the m controllable roll states $\mathbf{x}_{\mathrm{r,c}}$ and the uncontrollable roll states $\mathbf{x}_{\mathrm{r,u}}$. The matrices $\mathbf{A}$ and $\mathbf{B} = [\mathbf{B}_1 \mid \mathbf{B}_0]$ are partitioned correspondingly:

$$\begin{bmatrix} \mathbf{A}_{11} & \mathbf{A}_{12} & \mathbf{A}_{13} \\ \mathbf{A}_{21} & \mathbf{A}_{22} & \mathbf{A}_{23} \\ \mathbf{A}_{31} & \mathbf{A}_{32} & \mathbf{A}_{33} \end{bmatrix} \begin{bmatrix} \mathbf{x}_{\mathrm{h}} \\ \mathbf{x}_{\mathrm{r,c}} \\ \mathbf{x}_{\mathrm{r,u}} \end{bmatrix} + \left[\begin{array}{c|c} \mathbf{B}_{11} & \mathbf{B}_{12} \\ \mathbf{B}_{21} & \mathbf{B}_{22} \\ \mathbf{B}_{31} & \mathbf{B}_{32} \end{array}\right] \begin{bmatrix} \delta \\ \boldsymbol{u} \end{bmatrix} = \begin{bmatrix} 0 \\ 0 \\ 0 \end{bmatrix} \tag{17}$$

The active antiroll bar torques $\boldsymbol{u}$ have no effect on the steady state handling performance of the linearized system ($\mathbf{A}_{12} = \mathbf{A}_{13} = \mathbf{B}_{12} = 0$) and the handling states can be computed by

$$\mathbf{x}_{\mathrm{h}} = -\mathbf{A}_{11}^{-1}\mathbf{B}_{11}\delta \tag{18}$$

Functional controllability of the roll states can be verified by solving for the control inputs $\boldsymbol{u}$ as a function of the controlled roll states $\mathbf{x}_{\mathrm{r,c}}$:

$$\boldsymbol{u} = \mathbf{K}_{\mathrm{c}}\mathbf{x}_{\mathrm{r,c}} + \mathbf{K}_{\delta}\delta \tag{19}$$

where $\mathbf{K}_{\mathrm{c}}$ and $\mathbf{K}_{\delta}$ are matrices depending on the vehicle parameters. The roll states $\mathbf{x}_{\mathrm{r,c}}$ are functionally controllable if $\mathbf{K}_{\mathrm{c}}$ is not singular, and the values of the uncontrollable roll states $\mathbf{x}_{\mathrm{r,u}}$ can then be solved by back substitution. Full details have been given in reference [**18**].

That a system is functionally controllable implies that a set of control of inputs can influence a set of performance outputs to some extent. However input–output controllability may still be limited by other factors, including control input saturation, such as occurs at wheel lift-off.

3.3.2 *Roll stability and wheel lift-off*

Figure 5, discussed in section 3.2.2, shows that the lateral acceleration at which wheel lift-off first occurs is not necessarily a reliable indicator of the rollover threshold of the vehicle. It is important to establish the conditions under which the vehicle can retain roll stability even when some axles are off the ground and to understand the stabilizing mechanisms. The motivation is to identify the *critical* axles, the lift-off of which governs the rollover threshold.

To investigate the implications of wheel lift-off on vehicle roll stability, consider a linear vehicle model, of the type presented in section 2, but with two modifications:

1. The lateral load transfer at each axle is limited to a maximum value determined by the wheel lift-off condition.
2. The roll angle between the sprung and unsprung masses is limited to a maximum value determined by the available suspension travel.

3.3.3 *Roll stability without active roll control*

Firstly, consider the case of a vehicle fitted with a conventional passive suspension system. (The active case is examined in section 3.3.4.) When all load transfers are subcritical, at low levels of lateral acceleration, the linearized response of the vehicle is governed by

$$\dot{\boldsymbol{x}} = \mathbf{A}\boldsymbol{x} + \mathbf{B}_1\delta \tag{20}$$

where the matrices $\mathbf{A}$ and $\mathbf{B}_1$ are formed as in section 2. The stability of the system (both in roll and in handling) can be checked by verifying that the eigenvalues of $\mathbf{A}$ all lie in the open left half-plane.

If the steering inputs excite a response that causes the wheels at one or more axles to lift off, then equation (20) does not hold since the restoring moment at one or more axles reaches a limit. Beyond lift-off the vehicle response is governed by an equation of the form

$$\dot{\boldsymbol{x}} = \tilde{\mathbf{A}}\boldsymbol{x} + (\mathbf{A} - \tilde{\mathbf{A}})\tilde{\boldsymbol{x}} + \mathbf{B}_1\delta \tag{21}$$

The matrix $\tilde{\mathbf{A}}$ is a modified version of $\mathbf{A}$ with the tyre roll stiffness terms k_{t} set to zero at the lifted axles. This accounts for the fact that, after lift-off, an axle can no longer provide any additional restoring moment. The

* Additional control hardware designed to twist vehicle couplings or frames could be fitted to reduce but not to eliminate the plant input deficiency. Some judicious relaxation of the control objectives is necessary.

constant vector $\tilde{\boldsymbol{x}}$ is a modified version of $\boldsymbol{x}$ with the unsprung mass roll angles ϕ_t at the lifted axles set to the lift-off value ϕ_t^* and all other entries set to zero. See reference [**18**] for a complete example.

Since $(\mathbf{A}-\tilde{\mathbf{A}})\tilde{\boldsymbol{x}}$ is constant, the stability of the system (both in roll and in handling) can be checked by verifying that the eigenvalues of $\tilde{\mathbf{A}}$ all lie in the open left half-plane. Recall that roll stability is determined by the ability of the vehicle to generate an increase in net restoring moment to balance the increase in primary overturning moment caused by an increase in the steering input. For a vehicle with no active roll control system, the change in net restoring moment is the increase in the stabilizing roll moment generated by load transfers at the axles minus the destabilizing lateral displacement moment generated by the outboard shift of the sprung masses. Thus, for the vehicle to retain roll stability after wheel lift-off, the compliance of the couplings, frames and tyres and suspensions of the axles remaining on the ground must be sufficiently small that the destabilizing effect of the lateral displacement moment does not exceed the stabilizing effect of the lateral load transfer. This is shown as a positive slope of the net restoring moment curve in Fig. 5, for example.

This analysis can be used to check the stability of the vehicle with any combination of axle groups on or off the ground and provides a technique for identifying which axles must be on the ground for the vehicle to retain roll stability.

3.3.4 *Roll stability with active roll control*

Next consider the case of a vehicle with an active roll control system. When all load transfers are subcritical, the linearized response of the vehicle is governed by

$$\dot{\boldsymbol{x}} = \mathbf{A}\boldsymbol{x} + \mathbf{B}_0\boldsymbol{u} + \mathbf{B}_1\delta \tag{22}$$

where $\mathbf{B}_0\boldsymbol{u}$ represents the effect of the roll moments from the active antiroll bars (see section 2).

Again the roll stability of the vehicle is determined by the ability of the vehicle to generate a net restoring moment to balance the increase in primary overturning moment generated by an increase in steering input. By varying the control torques between the sprung and unsprung masses, the active roll control system can manipulate the axle load transfers and the body roll angles, thus controlling the net stabilizing moment. Specifically it is possible to increase the inward lean of the vehicle units, thus using the lateral displacement moment to provide a stabilizing effect within the limits of available suspension travel. (This assumes that the vehicle units whose wheels have lifted off are torsionally coupled to the vehicle units whose wheels remain on the ground or, equivalently, that control torques from vehicle units whose axles remain on the ground can influence the roll angles of the vehicle units whose wheels have lifted off.) Clearly, given a sufficient stabilizing effect from the lateral displacement moment, it is possible to nullify the destabilizing effect of the primary overturning moment and to stabilize the vehicle in roll.

Achievable roll stability is therefore limited by the ability of the active roll control system to provide a sufficient stabilizing lateral displacement moment such that the net restoring moment can balance the primary overturning moment. This ability is in turn limited by the maximum allowable suspension deflection. Once the maximum allowable deflection is reached, the stabilizing effect is limited to that which would be provided by infinitely stiff suspension springs holding the sprung masses at the maximum inward roll angle. By analogy with the passive case (section 3.3.3), the stability of the system can be checked by verifying that the eigenvalues of $\tilde{\mathbf{A}}$ all lie in the open left half-plane. In the active case, $\tilde{\mathbf{A}}$ is formed from $\mathbf{A}$ by (a) setting the tyre roll stiffness terms k_t at the lifted axles to zero (as before) and (b) setting the suspension roll stiffness terms k at the other axles towards infinity. Again, see reference [**18**] for a complete example.

Even if the axles on the ground provide sufficient moment to tilt the vehicle units into the turn at the maximum allowable angle, the vehicle will still be unstable after wheel lift-off if the compliance of the couplings, frames and tyres of the axles remaining on the ground is sufficiently large that the destabilizing effect of the lateral displacement moment exceeds the stabilizing effect of the lateral load transfer.

The roll stability of a vehicle may not depend on the lateral load transfers at *all* axles. If there is excessive torsional compliance in vehicle frames, couplings or tyres, then it is possible for one section of a combination vehicle to lose roll stability while the lateral load transfers at other axles remain subcritical.

It is important to control the lateral load transfers at these subcritical axles, since the control system cannot stabilize the vehicle once the lateral load transfers at these axles reach the critical value required for wheel lift-off.

3.3.5 *Roll moment distribution to maximize the rollover threshold of a tractor–semitrailer*

The net restoring moment is equal to the sum of the restoring moments at the axles due to lateral load transfer plus the sum of the stabilizing moments due to the lateral displacements of the sprung masses. Since in general it is not possible to maximize these two quantities simultaneously, some compromise is required. Two alternative options* for maximizing the rollover threshold of a tractor–semitrailer are now presented.

The example that will be used to illustrate these concepts is the tractor–semitrailer model (see section 2.2). In this case, the tractor frame was assumed to be

* These options are extreme, and are chosen to provide a clear insight into what is achievable, rather than to be practical.

torsionally rigid. Therefore the vehicle has five roll states (the sprung mass roll angles of the tractor and semitrailer, and the lateral load transfers at the tractor steer axle, the tractor drive axle and the semitrailer axles) and three controllable active antiroll bar torques (one at each of the three axle groups).

Case I: maximizing the restoring moment from the axles. The first option is to set the restoring moment of all axles to the maximum possible load transfer (which corresponds to their value at rollover). The steady state roll angle and normalized lateral load transfer* responses of a tractor–semitrailer employing such a control scheme are shown in Fig. 6.

The load transfer specification forms a full set of functionally controllable states $\mathbf{x}_{r,c}$ in equation (17). It is not possible to specify any of the sprung mass roll angles independently, but instead the sprung mass roll angles required to achieve this specification are dependent states $\mathbf{x}_{r,u}$ that are a function of the steering input.

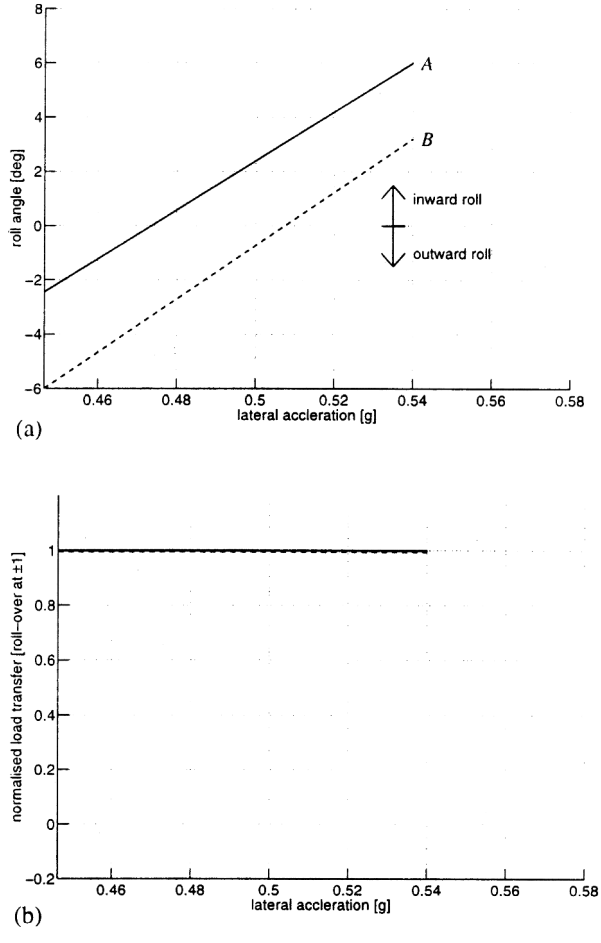

Fig. 6 Increasing the rollover threshold of the tractor–semitrailer by maximizing the stabilizing axle moment. (a) Suspension roll angles. Active roll control: tractor (——), semitrailer (– – –). (b) Normalized load transfers. Active roll control: tractor (——), semitrailer (– – –)

* The lateral load transfer is normalized such that a value of ± 1 corresponds to the maximum load transfer possible, i.e. lift off.

At low levels of lateral acceleration, this strategy requires that the vehicle is tilted *out* of the turn, which is clearly undesirable in practice. For lateral accelerations below 0.45*g*, it is not possible to lean this particular vehicle out of the turn enough to generate full load transfer at the axles because the semitrailer suspension reaches its limiting roll angle. At 0.45*g* it is possible to generate maximum load transfer at the tractor and semitrailer axles by tilting the tractor out of the turn by 2° and the semitrailer out of the turn by 6° (see Fig. 6a). As lateral acceleration increases, it is possible to maintain normalized load transfers of 1 by leaning the tractor and semitrailer progressively into the turn. The maximum allowable lateral acceleration corresponds to the vehicle state where the maximum inward sprung mass roll angle is equal to the maximum allowable roll angle. In this case, the tractor roll angle is 6° into the turn (point A), the semitrailer roll angle is 3.2° into the turn (point B) and the lateral acceleration at rollover is 0.54*g* (points A and B). The relative roll angle between the tractor and semitrailer reduces the load transfer on the semitrailer and increases the load transfer on the tractor. Although the restoring moment from the axles is maximized, the stabilizing lateral displacement moment is not.

It is possible that all sprung mass roll angles will reach the maximum allowable roll angle simultaneously, in which case the restoring moment and the stabilizing lateral displacement moment would be maximized simultaneously. However, in general this will not be the case and the relative roll angles between the sprung masses at rollover will be non-zero. These relative roll angles are normally needed to allow the total overturning moment to be shared among the axles to meet the control specification.

Case II: maximizing the stabilizing lateral displacement moment. The second option is to implement a scheme that sets the inward roll angle of the sprung mass at each axle to the maximum allowable roll angle. This maximizes the stabilizing effect of the lateral displacement moment. The steady state roll angle and normalized lateral load transfer responses of a tractor–semitrailer employing such a control scheme are shown in Fig. 7.

The roll angle specification forms a full set of functionally controllable states $\mathbf{x}_{r,c}$ in equation (17). It is not possible to specify any of the lateral load transfers independently, but instead the lateral load transfers required to achieve this specification are dependent states $\mathbf{x}_{r,u}$ that are functions of the steering input.

At very low levels of lateral acceleration, the inward lean of the tractor and semitrailer causes a small

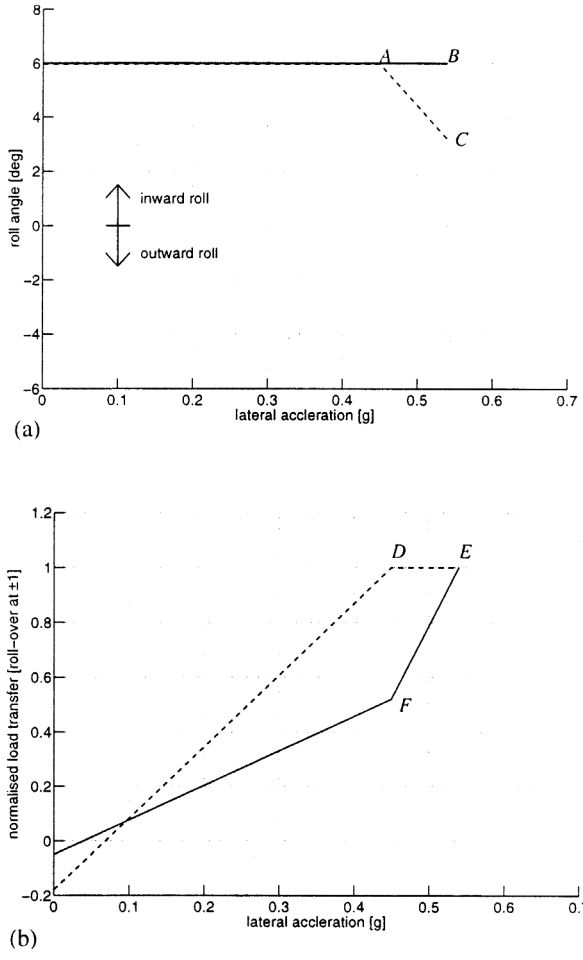

Fig. 7 Increasing the rollover threshold of the tractor–semitrailer by maximizing the stabilizing lateral displacement moment. (a) Suspension roll angles. Active roll control: tractor (——), semitrailer (– – –). (b) Normalized load transfers. Active roll control: tractor (——), semitrailer (– – –)

inward lateral load transfer. However, at modest levels of lateral acceleration (more than approximately 0.05*g*) the load transfer is towards the outside of the turn. When the lateral acceleration increases to 0.45*g*, load transfer reaches its maximum possible value at the semitrailer axles (point D) while the tractor axles still have significant additional load transfer capacity (point F). However, the lateral acceleration at which wheel lift-off first occurs is not a reliable indicator of the rollover threshold (see sections 3.2.2 and 3.3.2) because the vehicle can remain stable with a limited number of axles on the ground, subject to the stability conditions detailed in section 3.3.2.

As the lateral acceleration increases (see Fig. 6), the roll angle of the semitrailer cannot be maintained at the maximum value, and the roll angle decreases towards point C. This is because the wheel lift-off point sets a maximum value of control torque that can be generated at an axle, and so any additional overturning moment must cause a reduction in the inward sprung mass roll angle. Equivalently, since the restoring torque at the lifted axle reaches a maximum at wheel lift-off, then some roll angle outwards relative to the adjacent sprung masses is required to provide an additional stabilizing torque to balance any additional destabilizing overturning moment. Once the semitrailer axles lift off, the load transfer at the tractor axles increases rapidly until roll stability is lost at 0.54*g* (point E). By this point the semitrailer roll angle has been reduced to 3.2° (point C).

3.3.6 *Which strategy?*

Significantly, the vehicle states (load transfers and roll angles) at rollover for the two control schemes described above in case I and case II are identical, and both schemes yield the same rollover threshold. The techniques of maximizing the restoring moment and maximizing the stabilizing lateral displacement moment are therefore two different but equivalent ways of maximizing the rollover threshold. The following equivalent control strategies can therefore be used to maximize the roll stability of the vehicle:

(a) Balance the normalized load transfers at all critical axles while setting the maximum inward roll angle among the sprung masses to the maximum allowable angle.
(b) Maximize the inward roll angle of the sprung masses.

Control strategy (a) is preferable for several reasons:

1. Actuator force and power requirements are reduced.
2. Actuator bandwidth requirements are reduced.
3. The more progressive transition towards rollover minimizes the variation in handling characteristics.
4. An undesirable sign change in the roll rate response of the semitrailer is avoided.

The control inputs required to regulate these outputs may or may not include active antiroll bars at all axle groups. To maximize roll stability, active antiroll bars need only be fitted at axles from where they can exert some influence on the control outputs*. This can be verified by a functional controllability analysis from a reduced set of candidate control inputs to the new set of control outputs.

4 SIMULATION RESULTS

In order to demonstrate the achievable improvements to roll stability that can be obtained using active antiroll bars, roll control systems have been designed and

* It may be desirable to modify the control strategy for the steer axle so as to produce acceptable handling performance, possibly at the expense of some degradation of rollover threshold.

simulated for a range of heavy vehicles [**18**]. The results for a full-state feedback active roll control system for a tractor–semitrailer are presented here.

4.1 Control system design

The control system design techniques used to design active roll control systems have been detailed in full in reference [**18**]. The main ideas are as follows.

Since it is desirable to optimize the active roll control system across the range of possible steering inputs rather than simply in response to a single manoeuvre, the control system design problem is one of optimal disturbance rejection, where the disturbance to be rejected is the steering input from the driver.

The problem can be formulated as the synthesis of an optimal linear quadratic regulator in the presence of an exogeneous input (the steering). The steering input is described by a shaping filter ($\mathbf{A}_D, \mathbf{B}_D, \mathbf{C}_D, \mathbf{D}_D$) such that a zero-mean white-noise source w at the input to the filter produces an appropriately time correlated stochastic steering disturbance δ at the output:

$$\dot{\boldsymbol{x}}_D = \mathbf{A}_D \boldsymbol{x}_D + \mathbf{B}_D w, \qquad \delta = \mathbf{C}_D \boldsymbol{x}_D + \mathbf{D}_D w \tag{23}$$

Lin *et al.* developed a suitable steering spectrum by combining a low-frequency steering spectrum from UK road alignment data with a higher-frequency steering spectrum to represent lane change manoeuvres [**11**, **12**]. Combining the spectral densities from these low- and high-frequency sources, they found that, for a very active level of driver input on a typical road, the steering input spectrum could be modelled approximately by white noise filtered with a first-order filter with a cut-off frequency of 4 rad/s:

$$\dot{\boldsymbol{x}}_D = -4\boldsymbol{x}_D + 2w, \qquad \delta = 2\boldsymbol{x}_D \tag{24}$$

This steering disturbance δ then acts as the input to the vehicle system through the input injection node described by the matrix $\mathbf{B}_1$ such that the dynamics of the system are described by

$$\begin{aligned}\dot{\boldsymbol{x}} &= \mathbf{A}\boldsymbol{x} + \mathbf{B}_0\boldsymbol{u} + \mathbf{B}_1\delta \\ &= \mathbf{A}x + \mathbf{B}_0 u + \mathbf{B}_1\mathbf{C}_D x_D + \mathbf{B}_1\mathbf{D}_D w\end{aligned} \tag{25}$$

as shown in Fig. 8a.

Equation (25) can be rewritten by forming an augmented state vector $\underline{\boldsymbol{x}}$ including the system states $\boldsymbol{x}$ and the disturbance state $\boldsymbol{x}_D$ such that the dynamics of the system are described by

$$\dot{\underline{\boldsymbol{x}}} = \underline{\mathbf{A}}\underline{\boldsymbol{x}} + \underline{\mathbf{B}}_0\boldsymbol{u} + \underline{\mathbf{B}}_1 w \tag{26}$$

where

$$\underline{\boldsymbol{x}} = \begin{bmatrix}\boldsymbol{x} \\ \boldsymbol{x}_D\end{bmatrix}, \qquad \underline{\mathbf{A}} = \begin{bmatrix}\mathbf{A} & \mathbf{B}_1\mathbf{C}_D \\ 0 & \mathbf{A}_D\end{bmatrix}$$

$$\underline{\mathbf{B}}_0 = \begin{bmatrix}\mathbf{B}_0 \\ \mathbf{0}\end{bmatrix}, \qquad \underline{\mathbf{B}}_1 = \begin{bmatrix}\mathbf{B}_1\mathbf{D}_D \\ \mathbf{B}_D\end{bmatrix}$$

The optimal control is chosen to minimize the performance index

$$J = \int_0^\infty (\boldsymbol{z}^T\mathbf{Q}\boldsymbol{z} + \boldsymbol{u}^T\mathbf{R}\boldsymbol{u})\,\mathrm{d}t \tag{27}$$

where the matrices $\mathbf{Q}$ and $\mathbf{R}$ are design parameters representing the relative weighting of the performance output trajectory $\boldsymbol{z}$ and the control input $\boldsymbol{u}$ respectively.

The optimal controller is a feedback controller $\mathbf{K}_{FB}$ operating on $\underline{\boldsymbol{x}}$, and the optimal control law is given by

$$\boldsymbol{u}(t) = \mathbf{K}_{FB}\underline{\boldsymbol{x}}(t) \tag{28}$$

where

$$\mathbf{K}_{FB} = -\mathbf{R}^{-1}\underline{\mathbf{B}}_0^T\mathbf{S} \tag{29}$$

and where $\mathbf{S}$ is the solution to the appropriate Riccati equation [**18**]. The controller configuration is shown in Fig. 8b.

Partitioning the feedback controller $\mathbf{K}_{FB} = [\mathbf{K}_{FB,1}\ \ \mathbf{K}_{FB,2}]$ such that $\mathbf{K}_{FB,1}$ denotes the gain on $\boldsymbol{x}$ and $\mathbf{K}_{FB,2}$ denotes the gain on x_D, the closed-loop system is described by

$$\begin{bmatrix}\dot{\boldsymbol{x}} \\ \dot{\boldsymbol{x}}_D\end{bmatrix} = \begin{bmatrix}\mathbf{A} + \mathbf{B}_0\mathbf{K}_{FB,1} & \mathbf{B}_1\mathbf{C}_D + \mathbf{B}_0\mathbf{K}_{FB,2} \\ 0 & \mathbf{A}_D\end{bmatrix}\begin{bmatrix}\boldsymbol{x} \\ \boldsymbol{x}_D\end{bmatrix} + \begin{bmatrix}\mathbf{B}_1\mathbf{D}_D \\ \mathbf{B}_D\end{bmatrix} w \tag{30}$$

The term $\mathbf{B}_0\mathbf{K}_{FB,2}$ acts as a feedforward control on the disturbance states $\boldsymbol{x}_D$. This feedforward action reduces the response of the closed-loop system to stochastic disturbances. However, the stability of the closed-loop system is unaffected by this feedforward control since the closed-loop eigenvalues of the system are simply the eigenvalues of $\mathbf{A} + \mathbf{B}_0\mathbf{K}_{FB,1}$ and $\mathbf{A}_D$.

Effective disturbance rejection can be achieved if the dynamic properties of the disturbance are modelled and included in the controller design [**21**]. For an optimal disturbance rejection law, the states of the disturbance inputs must be measured or estimated such that the feedback of the disturbance states to the controller becomes part of the feedback law.

The weighting matrices $\mathbf{Q}$ and $\mathbf{R}$ penalize the performance output $\boldsymbol{z}$ and the control input $\boldsymbol{u}$ respectively. In order to simplify the selection of these matrices, the elements of $\mathbf{Q}$ are chosen to penalize only the unsprung mass roll angle terms (since the load transfer at an axle is equal to the unsprung mass roll angle multiplied by the effective roll stiffness of the tyres):

$$\boldsymbol{z} = [\phi_{t,f} \quad \phi_{t,r}]^T \tag{31}$$

The constraint on suspension roll angles is handled implicitly by selecting the elements of $\mathbf{R}$ to be sufficiently large to limit the roll moments from the active antiroll bars, since excessive roll moments lead to excessive inward roll angles. A useful starting point for selecting the elements of the weighting matrices is to choose $\mathbf{Q}$

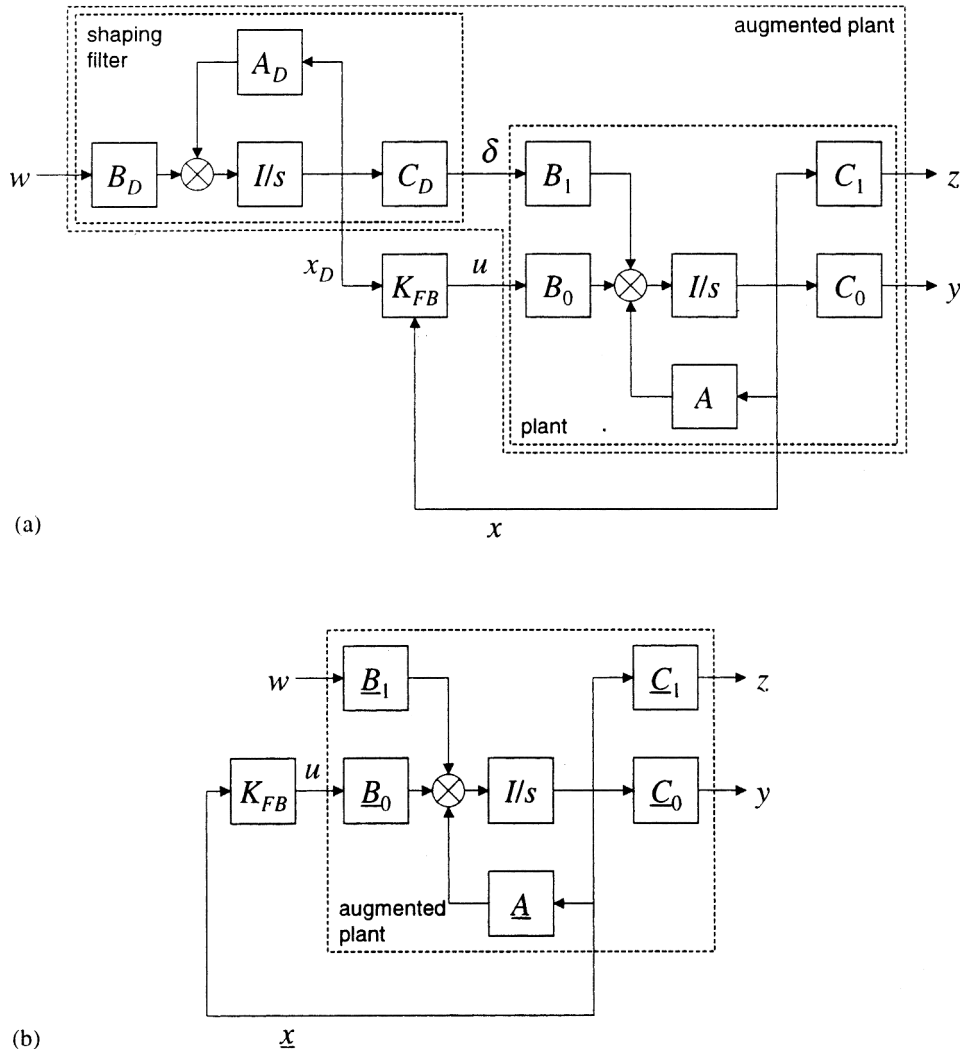

Fig. 8 Optimal disturbance rejection. (a) Detailed model showing the shaping filter and the plant. (b) Simplified model showing the augmented plant

and **R** as diagonal matrices:

$$\mathbf{Q} = \begin{bmatrix} q_1 & 0 \\ 0 & q_2 \end{bmatrix}, \qquad q_i = z_{i,\max}^{-2} \tag{32}$$

and

$$\mathbf{R} = \begin{bmatrix} r_1 & 0 \\ 0 & r_2 \end{bmatrix}, \qquad r_i = u_{i,\max}^{-2} \tag{33}$$

where $z_{i,\max}$ and $u_{i,\max}$ are the maximum acceptable values of the ith elements of the performance output vector and control input vector respectively [**22**]. From this starting point, an iterative design process follows in which the elements of **Q** and **R** are tuned to produce a controller with acceptable performance across a range of manoeuvres. The following tuning procedure was used for the vehicle investigated in this paper and for several other configurations [**18**], and produced good performance with a reasonably limited number of design iterations:

1. Adjust the elements of **Q** and **R** to tune the steady state performance of the system such that the normalized load transfers at all critical axles are balanced and the maximum inward suspension roll angle at rollover is around 4°. Although this may seem conservative, the largest steady state suspension roll angle should be less than the maximum allowable angle (approximately 5°) to leave space for overshoot in severe transient manoeuvres; otherwise the axles will strike the bump stops.
2. Simulate the performance of the vehicle for a range of severe transient manoeuvres including step steering inputs and lane changes.
3. If the maximum suspension roll angle in response to any critical* transient manoeuvre is greater than the maximum allowable angle, then step 1 should be

* A manoeuvre is described as *critical* when the size of the steering input is just sufficient to induce rollover.

repeated with the largest steady state inward suspension roll angle at rollover reduced.

4. If the peak normalized load transfer responses among the axles are poorly balanced in severe transient manoeuvres, it is necessary to adjust the elements of **Q** and **R**. This will necessarily require a compromise in the steady state balance. The compromise required is typically small for torsionally rigid single-unit vehicles. A greater compromise is required for articulated vehicles, particularly when a high level of rearward amplification is present, for example at high speeds or where pintle hitch couplings are used.

4.2 Vehicle description

The tractor–semitrailer combination consists of the two-axle tractor joined to a three-axle tanker semitrailer by a fifth-wheel coupling. The tractor and semitrailer parameters, which have been detailed in reference [**18**], are from an experimental vehicle that is currently being designed and built at the University of Cambridge. The control strategies developed here will be implemented and tested on this prototype vehicle.

The tractor unit has a wheelbase of 3.7 m, with single tyres on the steer axle and dual tyres on the drive axle. The unladen axle weights are 45 kN on the steer axle and 19 kN on the drive axle. The torsional stiffness of the vehicle frame is 629 kN m/rad.

The three axles of the semitrailer are spaced evenly at 1.31 m intervals, and the distance from the front axle centre-line to the fifth-wheel coupling is 6.39 m. Each axle is fitted with wide single tyres. The tanker body is significantly stiffer than the tractor frame, and the combined torsional stiffness of the tanker frame and the fifth-wheel coupling is 3000 kN m/rad. The unladen mass of the semitrailer is 5420 kg, and the unladen axle weights are 14 kN on each axle. The total mass of the laden semitrailer is 33 220 kg (including 27 800 l of water), and the laden axle weights are 80 kN on each axle.

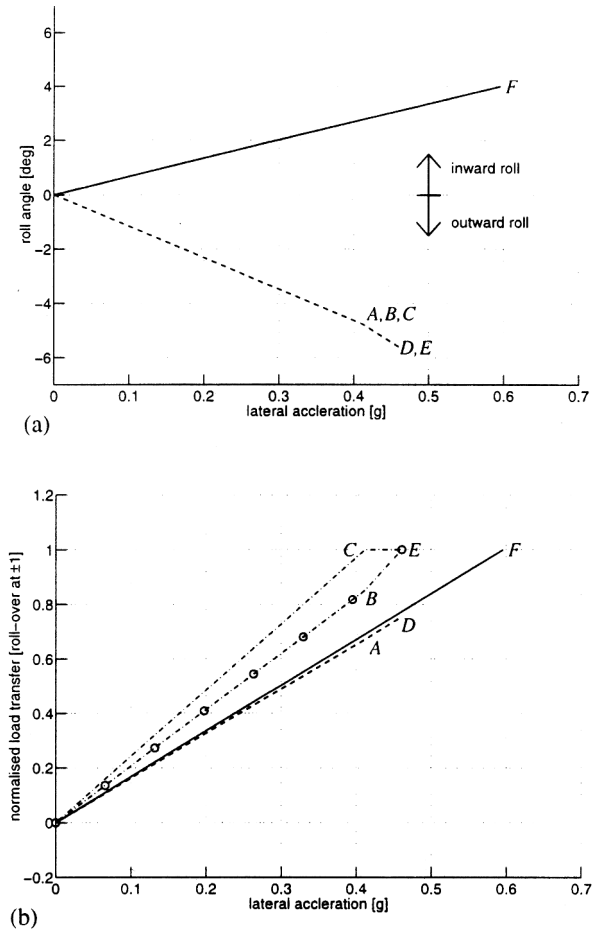

Fig. 9 Response of the linear, torsionally flexible tractor–semitrailer model with a passive suspension or a full-state feedback controller to a steady state steering input. (a) Suspension roll angles. Active roll control: steer axle (——); passive suspension: semitrailer axles (– – –). (b) Normalized load transfers. Active roll control: steer axle, drive axle and semitrailer axles (——); passive suspension: steer axle (– – –), drive axle (· – · – ·) and semitrailer axles (· – ○ – ·)

4.3 Steady state cornering response

The response of a linear model of the torsionally flexible tractor–semitrailer to a steady state steering input at 60 km/h is shown in Fig. 9. Without active roll control, the vehicle rolls out of the corner. The normalized load transfer builds up most quickly at the tractor drive axle and most slowly at the tractor steer axle, although this effect becomes more pronounced as torsional flexibility of the tractor frame increases. The drive axle lifts off at $0.41g$ (point C), at which point the normalized load transfer at the tractor steer axle is 0.67 (point A) and is 0.85 at the semitrailer axles (point B). As lateral acceleration continues to increase, the slopes of the suspension roll angle and normalized load transfer curves increase. The semitrailer axles lift off at $0.46g$ (point E), at which point the normalized load transfer at the steer axle is 0.76 (point D). Beyond this point, the steer axle is unable to stabilize the vehicle, and rollover occurs.

With active roll control, the vehicle rolls into the corner. The total roll moment is distributed among the active antiroll bars so that the normalized load transfers at all axles increase in a balanced fashion with lateral acceleration. This requires a relative roll angle of $4.0^\circ/g$ between the front and rear sections of the tractor unit (with the front section rolling into the corner more than the rear) and a relative roll angle between the rear section of the tractor unit and the rear section of the semitrailer of $1.2^\circ/g$ (with the tractor rolling into the corner more than the semitrailer). For greater frame flexibilities, the relative roll angles required to balance the normalized load transfers increase. The normalized load transfers at all axles reach the critical value of 1 simultaneously at

0.60g (point F), at which point the maximum inward suspension roll angle is 4.0° at the tractor steer axle.

Active roll control increases the rollover threshold of the torsionally flexible tractor–semitrailer by 29 per cent and the lateral acceleration at which axle lift-off first occurs by 45 per cent. This is a significant improvement in steady state roll stability.

4.4 Response to a step steering input

The response of the vehicle model to a step steering input is shown in Fig. 10. The step input is scaled to give a maximum normalized load transfer of 1 for the passive vehicle and the steady state lateral acceleration is 0.41g.

The suspension roll angle responses are shown in Fig. 10a. Without active roll control, the vehicle rolls out of the corner, with peak suspension roll angles of 3.7° at the tractor steer axle and 4.8° at the tractor drive and semitrailer axles. The active roll control system causes the vehicle to roll into the corner, with peak suspension roll angles of 3.0° at the tractor steer axle, 1.6° at the tractor drive axle and 2.2° at the semitrailer axles. The corresponding steady state suspension roll angles are 2.8°, 0.9° and 1.4°. Although the suspension roll angle is greater at the semitrailer axles than at the tractor drive axle, the absolute inward roll angle of the tractor's rear section is again actually greater than that of the semitrailer, the difference being due to the higher stiffness of the tractor tyres.

The normalized load transfer responses are shown in Fig. 9b. For the passive suspension, the normalized load transfer again builds up most rapidly at the tractor drive axle and most slowly at the tractor steer axle. This trend is more apparent for more flexible vehicle frames; i.e. frame flexibility reduces the ability of the tractor steer axle, in particular, to carry its share of the total lateral load transfer.

The normalized load transfer responses feature small overshoots before settling at final values of 0.67, 1.00 and 0.85 at the tractor steer, tractor drive and semitrailer axles respectively. In addition to reducing the total lateral load transfer by rolling the vehicle units into the turn, the active roll control system redistributes the load transfer in a balanced fashion among the axles so that all show a peak normalized value of 0.69 at all axles. The system reduces the peak load transfer by 31 per cent at the tractor drive axle and by 19 per cent at the semitrailer axles. The load transfer at the tractor steer axle remains essentially unchanged. However, rather than indicating poor controller performance, this emphasizes that the tractor steer axle carries much less than its 'fair share' of the total load transfer in the passive case.

The steady state results in section 4.3 show that, with passive suspension, the rollover threshold for this vehicle is 12 per cent higher than the lateral acceleration at which axle lift-off first occurs. However, with active roll

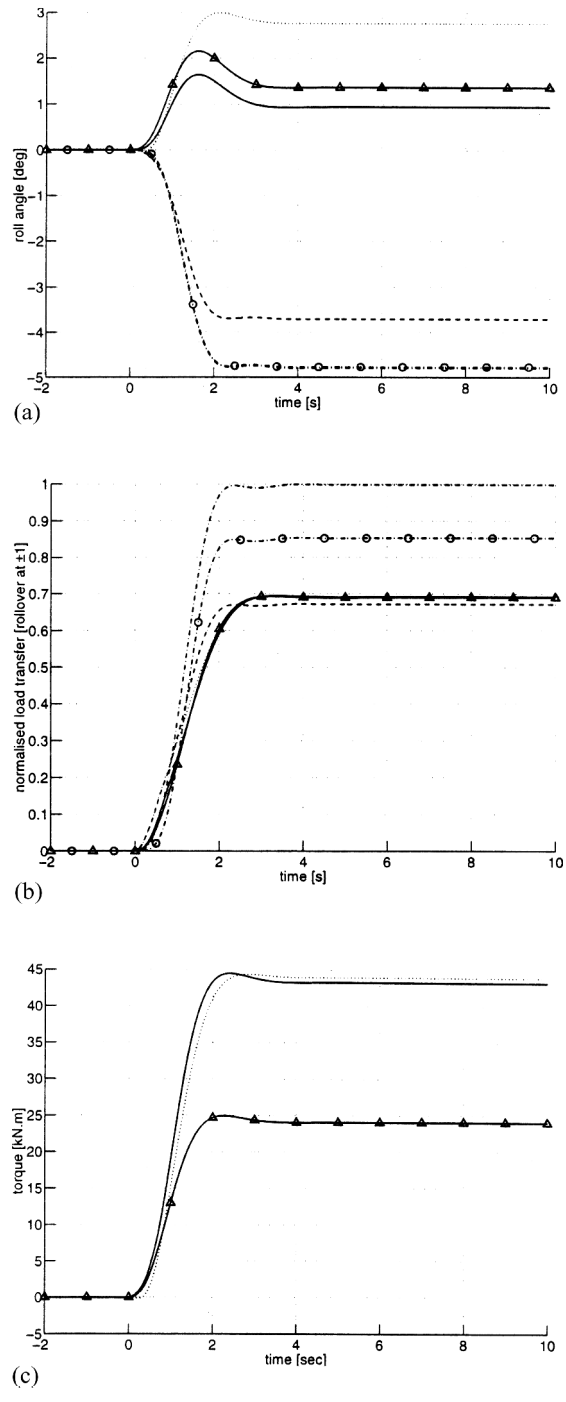

Fig. 10 Response of the linear, torsionally flexible tractor–semitrailer model with a passive suspension or a full-state feedback controller to a step steering input. (a) Suspension roll angles. Active roll control: steer axle (· · · · · ·), drive axle (——), semitrailer axles (——△——); passive suspension: steer axle (– – –), drive axle (· – · – ·), semitrailer axles (· – ○ – ·). (b) Normalized load transfers. Active roll control: steer axle (· · · · · ·), drive axle (——), semitrailer axles (——△——); passive suspension: steer axle (– – –), drive axle (· – · – ·), semitrailer axles (· – ○ – ·). (c) Active antiroll bar moments. Active roll control: steer axle (· · · · · ·), drive axle (——), semitrailer axles (——△——)

control, the vehicle can remain stable with up to 45 per cent additional lateral acceleration (i.e. up to 0.60*g*). This represents a significant improvement in roll stability. The peak inward suspension roll angle in response to such a critical manoeuvre is 4.3°, which is within the allowable limits.

The active antiroll bar moment responses are shown in Fig. 10c. The peak roll moment in response to a critical manoeuvre is 64 kN m at the drive axle. The roll moment builds up most quickly at the tractor drive and semitrailer axles to distribute the total load transfer evenly among the axles throughout the early part of this severe manoeuvre. The peak flowrate in response to a critical step manoeuvre is 0.78 l/s. The peak power supplied to the system in response to a critical step steering input, neglecting losses, is 6.9 kW.

4.5 Response to a double-lane change steering input

The response of the vehicle to a double-lane change steering input at 60 km/h is illustrated in Fig. 11 (see reference [**18**] for the definition of this manoeuvre). The path deviation over a 120 m test section is 5.05 m for the tractor and 5.2 m for the semitrailer. The peak lateral acceleration is 0.21*g*.

The suspension roll angle responses are shown in Fig. 11a. The trends discussed in sections 4.3 and 4.4 are again apparent. Active roll control causes the vehicle to roll into the corners, with the tractor unit rolling more towards the inside than the semitrailer.

The normalized load transfer responses are shown in Fig. 11b. In the passive case, the normalized load transfers are unbalanced, with the tractor drive axle bearing significantly more than its share of the total load transfer and the tractor steer axle bearing significantly less than its share. The peak load transfers are 0.28 at the tractor steer axle, 0.48 at the tractor drive axle and 0.43 at the semitrailer axles. When equipped with the active roll control system, the normalized load transfer responses are better balanced, with peak values of 0.30 at all axles. Peak normalized load transfer is reduced by 39 per cent at the tractor drive axle and 31 per cent at the semitrailer axles.

The peak inward roll angle at the semitrailer axles in response to a critical double-lane change steering input is 5.8°. This is within the available suspension travel.

Figure 11c illustrates that the largest active antiroll moment for this manoeuvre is 22 kN m at the tractor drive axle. The roll moment in response to a critical double-lane change steering input for which rollover would occur is therefore 73 kN m. The peak flowrate through the servo-valves is 0.51 l/s at the tractor steer axle. The peak power supplied to the system during a critical double-lane change, neglecting losses, is 25 kW.

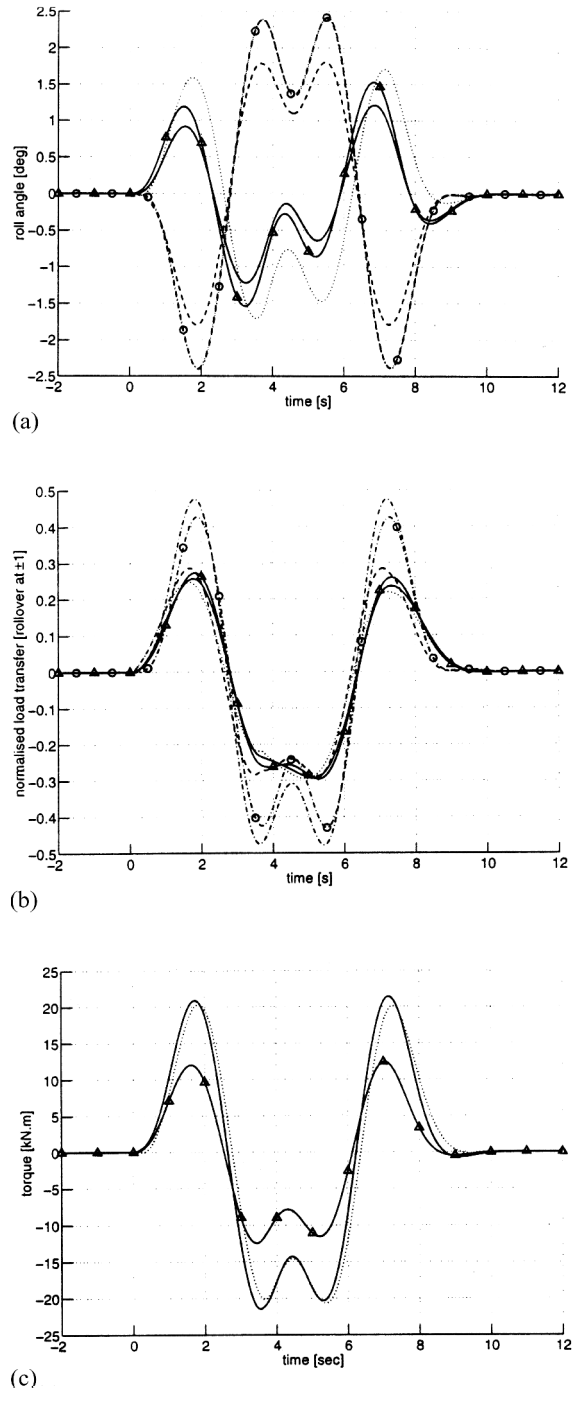

Fig. 11 Response of the linear, torsionally flexible tractor–semitrailer model with a passive suspension or a full-state feedback controller to a double-lane change steering input. (a) Suspension roll angles. Active roll control: steer axle (· · · · · ·), drive axle (——), semitrailer axles (——△——); passive suspension: steer axle (— — —), drive axle (· — · — ·), semitrailer axles (· — ○ — ·). (b) Normalized load transfers. Active roll control: steer axle (· · · · · ·), drive axle (——), semitrailer axles (——△——); passive suspension: steer axle (— — —), drive axle (· — · — ·), semitrailer axles (· — ○ — ·). (c) Active antiroll bar moments. Active roll control: steer axle (· · · · · ·), drive axle (——), semitrailer axles (——△——)

4.6 Effect on handling performance

The handling stability of a vehicle depends on the balance of tyre cornering stiffnesses among the axles. This balance changes with lateral load transfer because of the non-linear relationship between tyre cornering stiffness and vertical load. Since an active roll control system alters the distribution of lateral load transfer among the axles, it will impact the handling of the vehicle.

The effect of this active roll control system on the handling performance of the torsionally flexible tractor–semitrailer model at 60 km/h is shown in Fig. 12. This model included the non-linear tyre characteristics described in section 2.1. The handling responses of both the tractor and the semitrailer are included in the figure because the yaw stability of the combination is determined by the handling characteristics of both vehicle units [**16**].

First, consider the response of the vehicle without active roll control. At low levels of lateral acceleration, the tractor unit understeers mildly. As lateral acceleration increases, the normalized load transfer builds up more quickly at the drive axle than at the steer axle, an effect that is accentuated by reducing the torsional rigidity of the tractor frame. The handling balance of the tractor changes to mild oversteer by 0.2*g*. The tractor oversteers with increasing severity as lateral acceleration builds up. Yaw stability will be lost at high speed and high lateral acceleration if both the tractor and the semitrailer are oversteering [**16**].

Despite the presence of torsional flexibility in the tractor and semitrailer frames and in the fifth-wheel coupling, this active roll control system balances the build-up of normalized load transfer evenly between all the axles. The active roll control system causes the understeer gradient of the tractor to increase with increasing lateral acceleration and also reduces the severity of oversteer at the semitrailer. As long as the tractor unit understeers, the combination cannot be unstable in yaw [**16**]. Therefore, the active roll control system significantly increases yaw stability at high levels of lateral acceleration.

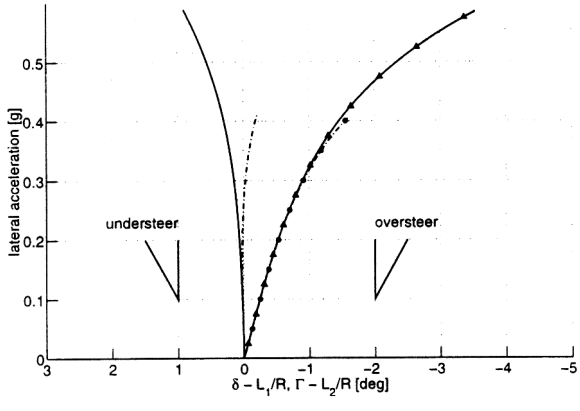

Fig. 12 Handling diagram of the torsionally flexible tractor–semitrailer with a passive suspension or a full-state feedback controller. Active roll control: tractor (——), semitrailer (—△—); passive suspension: tractor (· — · — ·), semitrailer axles (· —○— ·)

5 CONCLUSIONS

1. Achievable roll stability is limited because it is not possible to control all axle load transfers and body roll angles independently using active antiroll bars alone. The best achievable control objective for maximizing roll stability was shown to be setting the normalized load transfers at all critical axles to be equal while taking the largest inward suspension roll angle to be the maximum allowable angle.
2. Simulations showed that active roll control systems can increase the rollover threshold of a torsionally flexible tractor–semitrailer by 29 per cent. Such an improvement in roll stability represents a significant increase in vehicle safety.
3. By distributing the total normalized load transfer among all axles in a balanced fashion, active roll control tends to increase understeer for both units of a typical tractor–semitrailer, thus increasing yaw stability.

ACKNOWLEDGEMENTS

The authors wish to acknowledge the financial support of the Cambridge Vehicle Dynamics Consortium and the Engineering and Physical Sciences Research Council. At the time of writing, the Cambridge Vehicle Dynamics Consortium consisted of the University of Cambridge and Cranfield University together with the following industrial partners from the European heavy-vehicle industry: Tinsley Bridge Limited, ArvinMeritor, Koni BV, Qinetiq, Pirelli, Shell UK Limited, Volvo Global Trucks, General Trailers, Firestone Industrial Products, Mektronika Systems and Fluid Power Design. Dr Sampson would like to thank the Cambridge Australia Trust and the Committee of Vice-Chancellors and Principals of the Universities of the United Kingdom for their support.

REFERENCES

1 **Blower, D.** and **Pettis, L.** Trucks involved in fatal accidents. Codebook 1996. Technical Report UMTRI-98-14, University of Michigan Transportation Research Institute, Ann Arbor, Michigan, 1998.
2 **Blower, D.** and **Pettis, L.** Trucks involved in fatal accidents. Codebook 1997. Technical Report UMTRI-99-18, University of Michigan Transportation Research Institute, Ann Arbor, Michigan, 1999.
3 **Von Glasner, E.-Ch.** Active safety of commercial vehicles.

In Proceedings of the 2nd International Symposium on *Advanced Vehicle Control*, Tsukuba, Japan, 1994, pp. 9–14.

4 **Winkler, C. B., Blower, D., Ervin, R. D.** and **Chalasani, R. M.** *Rollover of Heavy Commercial Vehicles*, 2000 (Society of Automotive Engineers, Warrendale, Pennsylvania).

5 **Winkler, C. B.** and **Ervin, R. D.** On-board estimation of the rollover threshold of tractor semitrailers. In Proceedings of the 16th IAVSD Symposium on *the Dynamics of Vehicles on Roads and Tracks*, Pretoria, South Africa, 1999, pp. 540–551.

6 **Winkler, C. B., Bogard, S. E., Ervin, R. D., Horsman, A., Blower, D., Mink, C.** and **Karamihas, S.** Evaluation of innovative converter dollies. Technical Report UMTRI-93-47, University of Michigan Transportation Research Institute, Ann Arbor, Michigan, 1993.

7 **Winkler, C. B.** and **Ervin, R. D.** Rollover of heavy commercial vehicles. Technical Report UMTRI-99-19, University of Michigan Transportation Research Institute, Ann Arbor, Michigan, 1999.

8 **Kusahara, Y., Li, X., Hata, N.** and **Watanabe, Y.** Feasibility study of active roll stabilizer for reducing roll angle of an experimental medium-duty truck. In Proceedings of the 2nd International Symposium on *Advanced Vehicle Control*, Tsukuba, Japan, 1994, pp. 343–348.

9 **Pflug, H. C., von Glasner, E.-Ch.** and **Povel, R.** Improvement of commercial vehicles' handling and stability by smart chassis systems. In *Smart Vehicles* (Eds J. P. Pauwelussen and H. B. Pacejka), 1995, pp. 318–338 (Swets and Zeitlinger, Lisse).

10 **Dunwoody, A. B.** and **Froese, S.** Active roll control of a semi-trailer. *SAE Trans.*, 1993, **102**(933045), 999–1004.

11 **Lin, R. C.** An investigation of active roll control for heavy vehicle suspensions. PhD thesis, University of Cambridge, Cambridge, 1994.

12 **Lin, R. C., Cebon, D.** and **Cole, D. J.** Optimal roll control of a single-unit lorry. *Proc. Instn Mech. Engrs, Part D, Journal of Automobile Engineering*, 1996, **201**(D1), 44–55.

13 **Lin, R. C., Cebon, D.** and **Cole, D. J.** Active roll control of articulated vehicles. *Veh. System Dynamics*, 1996, **26**(1), 17–43.

14 **Lin, R. C., Cebon, D.** and **Cole, D. J.** Validation of an articulated vehicle yaw/roll model. Technical Report CUED/C-MECH/TR 53, Department of Engineering, University of Cambridge, Cambridge, 1993.

15 **Segel, L.** Theoretical prediction and experimental substantiation of the response of an automobile to steering control. *Proc. Instn Mech. Engrs, Automotive Division*, 1956–57, pp. 310–330.

16 **Segel, L.** (Ed.) *Course on the Mechanics of Heavy-Duty Trucks and Truck Combinations*, 1988 (University of Michigan Transportation Research Institute, Surfers Paradise, Queensland).

17 **Fancher, P. S., Ervin, R. D., Winkler, C. B.** and **Gillespie, T. D.** A factbook of the mechanical properties of the components for single-unit and articulated heavy trucks. Technical Report UMTRI-86-12, University of Michigan Transportation Research Institute, Ann Arbor, Michigan, 1986.

18 **Sampson, D. J. M.** Active roll control of articulated heavy vehicles. PhD thesis, University of Cambridge, Cambridge, 2000.

19 **Cooperrider, N. K., Thomas, T. M.** and **Hammoud, S. A.** Testing and analysis of vehicle rollover behavior. *SAE Trans.*, 1990, **99**(900366), 518–527.

20 **Rosenbrock, H. H.** *State-Space and Multivariable Theory*, 1970 (Nelson, London).

21 **Lin, C.-F.** *Advanced Control Systems Design*, 1994 (Prentice-Hall, Upper Saddle River, New Jersey).

22 **Bryson, A. E.** and **Ho, Y. C.** *Applied Optimal Control*, 2nd edition, 1975 (Blaisdell, Waltham, Massachusetts).